

See discussions, stats, and author profiles for this publication at: <https://www.researchgate.net/publication/267024010>

Close-Packed Dye Molecules in Zeolite Channels Self-Assemble into Supramolecular Nanoladders

ARTICLE *in* THE JOURNAL OF PHYSICAL CHEMISTRY C · JANUARY 2014

Impact Factor: 4.77

CITATIONS

2

READS

28

9 AUTHORS, INCLUDING:



Rossella Arletti

Università degli Studi di Torino

86 PUBLICATIONS 516 CITATIONS

[SEE PROFILE](#)



Gianmario Martra

Università degli Studi di Torino

244 PUBLICATIONS 5,520 CITATIONS

[SEE PROFILE](#)



Simona Quartieri

Università degli Studi di Messina

132 PUBLICATIONS 1,820 CITATIONS

[SEE PROFILE](#)



Giovanna Vezzalini

Università degli Studi di Modena e Reggio E...

144 PUBLICATIONS 1,585 CITATIONS

[SEE PROFILE](#)

Close-Packed Dye Molecules in Zeolite Channels Self-Assemble into Supramolecular Nanoladders

Lara Gigli,[†] Rossella Arletti,^{‡,§} Gloria Tabacchi,^{*,||} Ettore Fois,^{||} Jenny G. Vitillo,^{§,||} Gianmario Martra,^{§,⊥} Giovanni Agostini,^{§,⊥,○} Simona Quartieri,[#] and Giovanna Vezzalini[†]

[†]Dipartimento di Scienze Chimiche e Geologiche, Università degli Studi di Modena e Reggio Emilia, Via Giuseppe Campi 183, 41125-Modena, Italy

[‡]Dipartimento di Scienze della Terra, Università degli Studi di Torino, Via Valperga Caluso 35, 10125-Torino, Italy

[§]Interdepartmental Centre “Nanostructure Interfaces and Surfaces—NIS”, Via Pietro Giuria 7, 10125-Torino, Italy

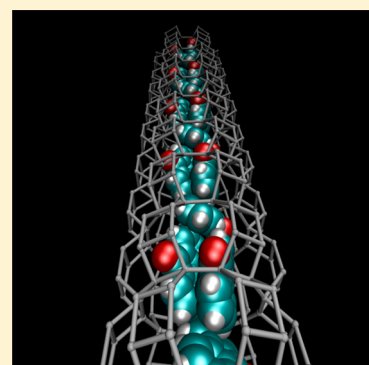
^{||}Dipartimento di Scienza ed Alta Tecnologia, Università degli Studi dell’Insubria, Via Lucini 3, 22100-Como, Italy

[⊥]Dipartimento di Chimica, Università degli Studi di Torino, Via Pietro Giuria 7, 10125-Torino, Italy

[#]Dipartimento di Fisica e Scienze della Terra, Università degli Studi di Messina, Viale Ferdinando Stagno d’Alcontres 3, 98166-Messina S.Agata, Italy

Supporting Information

ABSTRACT: A tough challenge in nanomaterials chemistry is the determination of the structure of multicomponent nanosystems. Dye–zeolite L composites are building blocks of hierarchically organized multifunctional materials for technological applications. Supramolecular organization inside zeolite L nanochannels, which governs electronic properties, is barely understood. This is especially true for confined close-packed dye molecules, a regime not investigated in applications yet and that might have great potential for future development in this field. Here we realize for the first time composites of zeolite L with maximally packed fluorenone molecules and elucidate their structure by integrated multitechnique analyses. By IR spectroscopy, thermogravimetric analysis, and X-ray diffraction, we establish the maximum degree of dye loading obtained (1.5 molecules per unit cell), and by modeling we reveal that at these conditions fluorenone molecules form quasi 1-D supramolecular nanoladders running along the zeolite channels. Spatial and morphological control provided by the nanoporous matrix combined with a complex blend of strong dye–zeolite and weaker dye–dye van der Waals interactions lie at the origin of this unique architecture, which is also stabilized by the hydrogen bond network of coadsorbed water molecules surrounding the dye nanoladder and penetrating between its rungs.



1. INTRODUCTION

Zeolites, beside their well-established use as catalysts and molecular sieves, are becoming increasingly popular in the cutting-edge field of design and fabrication of advanced functional materials.¹ The regular pore systems of nanometric openings exhibited by the framework make zeolites ideal host matrices for achieving supramolecular organization of photoactive species, leading to versatile building blocks for the realization of hierarchically organized multifunctional composite materials.^{1–3} Microlasers, pigments, optical switches, or artificial antenna systems are only few of the possible applications of these fascinating systems.^{4–10} To date, different zeolites with suitable channel dimensions, such as AlPO4-5,^{11,12} zeolite Y,¹³ and zeolite L,^{14,15} as well as mesoporous materials, such as MCM-41,¹⁶ have been successfully adopted as nanosized host matrices for the synthesis of these composites. In this rapidly evolving scenario, the inclusion of photoactive molecules into one-dimensional channel systems is of paramount relevance for further progress in some of the most challenging fields of nanoscience and nanotechnology. Since

the nanometric diameter channels of zeolites may induce an anisotropic arrangement of photoactive molecules, the resulting host–guest materials show outstanding energy transfer capabilities, mimicking the functionalities of the antenna systems of living plants.^{17–21} This is a key requirement for the fabrication of increasingly sophisticated optical devices which might open novel pathways in areas such as solar energy harvesting, information processing, and nanodiagnostics.^{22–24}

Zeolite L (ZL) is a very appealing host matrix for the realization of one-dimensional photoactive domains. Due to the narrow openings (free diameter 7.8 Å) and maximum diameter (~12 Å) of its channels, sufficiently bulky dye molecules are constrained to align to the channel axis and are prevented from passing each other. Moreover, ZL crystal growth is not affected by stacking fault problems that might occlude the parallel channel system.^{25,26} By virtue of such a feature, it is indeed

Received: April 4, 2014

Revised: July 1, 2014

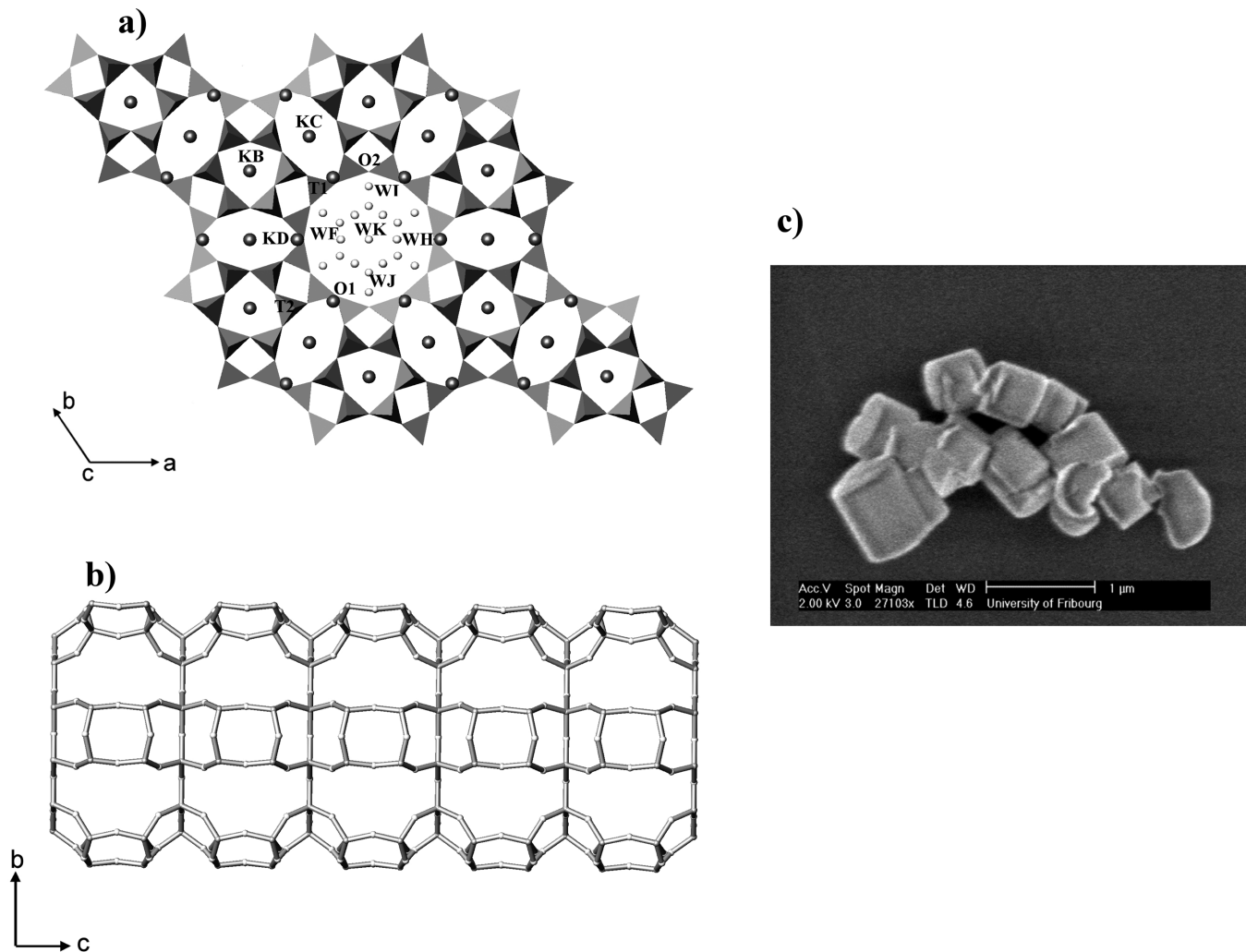


Figure 1. (a) Projection along [001] of zeolite L structure. Light gray: water sites; dark gray: K sites. (b) Side view of the 12 MR channel running along the *c* axis. (c) SEM picture of as-synthesized zeolite L crystals.

possible to obtain high concentrations of well oriented dye molecules, which are crucial for realizing, e.g., artificial antenna systems. An atomistic-detail knowledge of these organized arrangements of dyes would be fundamental for the future development of molecular-based optical devices.

Supramolecular organization in ZL nanochannels largely depends, at a microscopic level, on the orientation of the molecules with respect to the channel axis, which in turn depends on the size, shape, charge, and concentration of the photoactive guests, as well as on the presence and nature of the adopted cosolvent medium.¹ In addition, molecular packing plays a key role in modulating the dye orientation and, therefore, the properties of the composites, especially when dye molecules significantly smaller than the ZL channel aperture are included.^{1,3} In this case, the molecules are no longer constrained to align to the channel axis: due to the larger orientation freedom, their distribution is not uniform and their orientation depends on the local concentration. In such conditions, it becomes extremely difficult to predict the structural details of the supramolecular arrangement inside ZL simply on the basis of the geometrical parameters of the guest molecules.^{2,3}

Experimental information might be gathered by structural X-ray diffraction studies. However, in the case of dye-ZL systems,

difficulties arise from the high symmetry of the zeolite, from the low amount of the light atoms of the dye (which do not allow the determination of a possible symmetry lowering), and from the noncoincidence of the point symmetry of ZL with that of the dye. In addition, because of the nonuniform concentration/orientation of the dye, disorder along the channel could also be present. Furthermore, due to the small size of available ZL crystallites, single crystal X-ray diffraction is not affordable.²⁷ As a consequence, X-ray structural determinations on this kind of materials are extremely challenging: as a matter of fact, only a few diffraction studies are available in the literature.^{28,29}

Some insight can be provided by optical spectroscopy of oriented dye-ZL monolayers^{30,31} or by fluorescence microscopy approaches.^{32–34} Since both techniques probe the orientation of the electronic transition dipole moment of the molecules with respect to the ZL channel axis, only indirect information on the actual geometrical features of supramolecular organization can be obtained. Moreover, data interpretation is not straightforward because even single crystal microscopy data are the result of averaging over a large number of situations (e.g., a 600 nm diameter ZL crystal contains roughly 100 000 parallel channels)¹ stemming from the nonuniform orientation of the molecules. In this context, modeling dye-ZL composites could be of great help for

understanding the organization of molecules confined in nanochannels. For example, theoretical investigations on xanthene dye-ZL composites unraveled the orientation of the dye and revealed that it was influenced by the water cosolvent.³⁵ On the other hand, in the case of the dye fluorenone (FL), orientation was found to be governed by the strong interaction between the ZL extraframework potassium cations and the fluorenone carbonyl oxygen. Such an interaction was responsible for the stability of the fluorenone-ZL composite as well as for its substantial anisotropy, independent of the water content inside the channels.^{36,37}

All of these studies were performed by modeling a low dye loading in order to mimic the dye concentrations generally adopted in actual dye-ZL composites, which are normally below 0.5 molecules per unit cell.²³ The structure, properties, and behavior of highly packed dye-ZL materials, i.e., characterized by a high degree of dye loading, have never been explored to date, neither by experiment nor by modeling. A deep understanding of this regime might provide novel ideas and alternative routes for advances in the fabrication of ZL-based devices, and this work represents the first contribution toward this goal.

By exploiting the full potential of a multitechnique integrated experimental-computational approach, here we study for the first time high dye-loading ZL/FL materials and shed light on how dye molecules are organized in closely packed ZL/FL systems. In the following, the results of combined X-ray diffraction/IR/thermogravimetric analyses on ZL/FL systems characterized by different FL content are reported, discussed, and rationalized by theoretical modeling on the basis of a complex balance of interactions among dye molecules, water, and ZL matrix.

2. EXPERIMENTAL SECTION

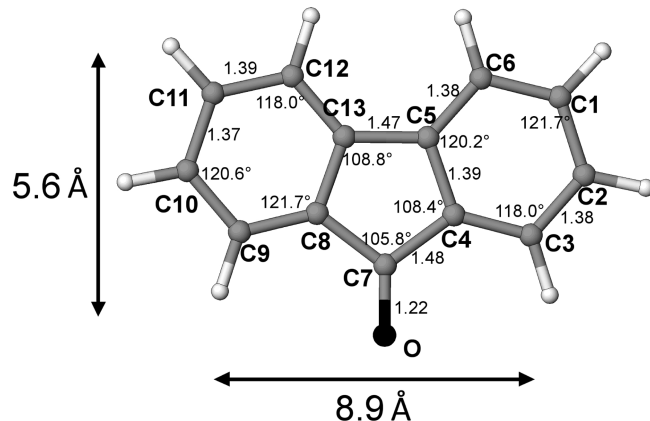
2.1. Materials. Host. Potassium zeolite L (LTL-framework type,²⁶ Si/Al ratio 2.9) was purchased from Tosoh Corporation (Japan) (code HSZ-500). The LTL framework (space group $P6/mmm$) is built of columns of cancrinite cages stacked with double six membered rings (D6R) along the c axis. These columns are connected to form large circular 12-ring (12MR) channels of size $7.4 \times 7.8 \text{ \AA}$ and smaller elliptical 8-ring (8MR) ones of $1.9 \times 5.6 \text{ \AA}$, both running along the c axis. The main channels are connected to the parallel 8MR ones by nonplanar boat-shaped 8 membered rings (Figure 1a,b).

The scanning electron microscopy (SEM) picture in Figure 1c shows the typical barrel shape of the crystals and a rather homogeneous size distribution of about $400 \times 600 \text{ nm}$. The chemical composition of the zeolite was determined by X-ray fluorescence and thermogravimetric analysis. The resulting chemical formula is $\text{K}_{8.46}(\text{Al}_{8.35}\text{Si}_{27.53})\text{O}_{72.17.91}\text{H}_2\text{O}$.

The XRPD pattern of the as-synthesized ZL (Figure S1 in the Supporting Information, hereafter SI) confirms the good crystallinity of the material and the absence of impurities.

Guest. 9-Fluorenone ($\text{C}_{13}\text{H}_8\text{O}$), purchased as an analytical standard by Sigma-Aldrich with a purity of 98.0%, was used without further purification. The dye is a neutral and flat organic molecule, with a carbonyl as functional group.³⁸ In Figure 2 the structure and the dimensions of the molecule are shown.

Synthesis of ZL/FL Composites. FL was inserted into the channels of ZL by using gas-phase adsorption. Four ZL/FL samples were synthesized with nominal loadings of 0.5, 1.0, 1.5, and 2.25 molecules per unit cell, following the experimental set



Data were collected in the 2θ range $3\text{--}120^\circ$ with steps of 0.02 and at 5.5 s per step speed.

The structural refinements of selected samples (as-synthesized ZL, ZL/0.5FL, ZL/1.0FL, and ZL/1.5FL) were based on high-resolution XRPD patterns collected at the SNBL (BM01a) beamline at ESRF (European Synchrotron Radiation Facility) in transmission geometry, with a fixed wavelength of 0.6825 \AA . The powder samples were loaded and packed in a 0.3 mm boron capillary, mounted on a standard goniometric head, and spun during data collection. Bidimensional diffraction patterns were recorded on a PILATUS3M-Series detector (pixel dimension $172\text{ }\mu\text{m}$) at a fixed distance of 193 mm from the sample. One-dimensional diffraction patterns were obtained in the 2θ range $0\text{--}50^\circ$ by integrating the two-dimensional images with the program FIT2D.⁴⁰

Structural Refinements. Structural refinements were performed by full profile Rietveld analysis using the GSAS package⁴¹ with the EXPGUI interface.⁴² Since no evidence of superstructure and symmetry change in the ZL/FL composites was detected from the analysis of the powder patterns, the refinements were performed in the $P6/mmm$ space group. The framework and potassium atom coordinates reported in ref 39 for the room temperature refinement were used as a starting model. For all tetrahedral atoms, the Si scattering factor was used, neglecting the amount of Al atoms. The Bragg peak profile was modeled using a pseudo-Voigt function with 0.01% cutoff peak intensity. The background was empirically fitted using a Chebyshev polynomial with 20 variable coefficients. The scale factor, 2θ -zero shift, and unit-cell parameters were accurately refined. Table 1 reports the refinement parameters

Table 1. Experimental and Refinement Parameters for ZL and for the ZL/0.5FL, ZL/1.0FL, and ZL/1.5FL Composites

| samples | ZL | ZL/0.5FL | ZL/1.0FL | ZL/1.5FL |
|---------------------|--------------|--------------|--------------|--------------|
| space group | $P6/mmm$ | $P6/mmm$ | $P6/mmm$ | $P6/mmm$ |
| $a\text{ (\AA)}$ | $18.3795(4)$ | $18.3860(6)$ | $18.3940(6)$ | $18.4211(7)$ |
| $c\text{ (\AA)}$ | $7.5281(2)$ | $7.5228(3)$ | $7.5203(3)$ | $7.5117(4)$ |
| $V\text{ (\AA}^3)$ | $2202.4(1)$ | $2202.4(1)$ | $2203.5(1)$ | $2207.5(2)$ |
| $R_p\text{ (%)}$ | 2.8 | 3.0 | 2.9 | 3.1 |
| $R_{wp}\text{ (%)}$ | 3.8 | 4.2 | 4.2 | 4.3 |
| RF**2 (%) | 7.3 | 7.5 | 7.8 | 8.7 |
| no. of variables | 73 | 84 | 81 | 107 |
| no. of observations | 1319 | 1187 | 1319 | 1187 |
| no. of reflections | 944 | 726 | 946 | 729 |

for ZL and for three composites. The thermal displacement parameters were constrained in the following way: the same value for all the tetrahedral atoms, a second value for all the framework oxygen atoms, a third one for the oxygen atoms of water molecules, and a fourth one for the FL molecule atoms. The thermal parameters of the K sites were allowed to vary. Occupancy factors and isotropic thermal displacement factors were refined in alternate refinement cycles. In the ZL/FL samples, the water and FL molecules were located after the inspection of the Fourier difference maps. H atoms were not considered during the structure refinement due to their low scattering factors. Soft constraints were imposed on tetrahedral bond lengths ($\text{Si}-\text{O} = 1.63\text{ \AA}$) as well as on the C-C (in the range $1.39\text{--}1.48\text{ \AA}$) and C-O (1.22 \AA) distances, with tolerance values of 0.03 \AA . These latter constraints could not be removed without unrealistic bond distances emerging in the

structure due to the high number of variables in the refinement and to the extremely low scattering power of the FL molecules; hence, the weight on the constraints was kept at a value of 1000 in the last cycles of the refinements. The occupancy of FL carbon sites was allowed to vary in the first refinement cycles and successively was fixed to the average value.

The final atomic positions and thermal parameters for the four refinements are given in Table S1. The framework and extraframework interatomic distances for ZL and for the composites are reported in Tables S2 and S3. The final observed and calculated powder patterns of as-synthesized ZL and of the ZL/0.5FL, ZL/1.0FL, and ZL/1.5FL composites are shown in Figure S1.

Models and Calculations. Density functional theory (DFT) calculations were performed on a series of models for the ZL/1.0FL and ZL/1.5FL composites. The PBE approximation⁴³ with periodic boundary conditions and Grimme corrections⁴⁴ for the FL-FL interactions was applied throughout. For both systems the simulation cell was twice the experimental unit cell (u.c.) of the ZL host along c . Calculations on the ZL/0.5FL composite (simulation cell stoichiometry: $K_{18}[\text{Al}_{18}\text{Si}_{54}\text{O}_{144}] \cdot \text{FL}$) with the PBE functional and periodic boundary conditions were previously performed and thoroughly described in refs 36 and 37.

Electronic wave functions were expanded in planewaves up to a kinetic energy cutoff of 25 Ry (200 Ry for the density). Electron-ionic core interactions were computed with ultrasoft Vanderbilt pseudopotentials for H, C, and O and with norm conserving pseudopotentials for Si, Al, and K (semicore in the case of K).⁴⁵⁻⁴⁸ This electronic structure computational scheme provided a proper description of the ZL/0.5FL composite,^{36,37} as well as of other large organic-inorganic systems.^{49-54,35} All calculations were performed with the CPMD code,⁵⁵ a particularly valuable approach in the study of quasi one-dimensional supramolecular systems inside zeolite nanochannels.⁵⁶⁻⁵⁹

In order to try establishing which close-packing arrangements of FL molecules could be possible inside ZL channels, dry ZL/FL models were first considered. Local energy minima for the dry ZL/1.0FL and ZL/1.5FL models, characterized by the simulation cell stoichiometries $K_{18}[\text{Al}_{18}\text{Si}_{54}\text{O}_{144}] \cdot 2\text{FL}$ and $K_{18}[\text{Al}_{18}\text{Si}_{54}\text{O}_{144}] \cdot 3\text{FL}$, respectively, were obtained by geometry optimization of different guess configurations. The guess configurations for the ZL/1.0FL and ZL/1.5FL systems were built by inserting two and three FL molecules per simulation cell, respectively (convergence criterion: $5 \times 10^{-4}\text{ au}$ for forces on atoms). In the ZL/1.5FL model, one ZL unit cell contained 2 FL molecules and the adjacent one 1 FL molecule. In the case of the ZL/1.0FL system, two different models were considered: model 1-1, characterized by an occupancy of 1 FL molecule per ZL unit cell, and model 2-0, where one ZL unit cell contained 2 FL molecules and the adjacent one 0 FL molecules. The guess geometries of both the 1-1 and 2-0 models were built by positioning the FL molecules so that their C=O groups were either in a parallel ("sin") or antiparallel ("anti") configuration. In all cases, the stabilization energy of the composites with respect to the isolated ZL and FL components was calculated with eq 1:

$$\Delta E(\text{ZL}\cdot n\text{FL}) = E(\text{ZL}\cdot n\text{FL}) - E(\text{ZL}) - n \times E(\text{FL}) \quad (1)$$

where $E(\text{ZL}\cdot n\text{FL})$ is the energy of the optimized dry ZL/nFL model ($n = 2, 3$ for ZL/1.0FL and ZL/1.5FL, respectively) and $E(\text{ZL})$ is the energy of the empty ZL, while $E(\text{FL})$ is the energy

of an isolated FL molecule calculated in the same simulation cell.

In the case of the low-FL-content system, i.e., the ZL/0.5FL composite, an atomistic-level structural description was obtained from both 0 K energy minimization and room temperature first-principles molecular dynamics trajectories, as discussed in ref 36, to which we refer for further details.

Once the minimum energy structure of the dry ZL/1.5FL system, corresponding to the maximum degree of FL loading, was obtained, several hydrated models characterized by stoichiometry $K_{18}[Al_{18}Si_{54}O_{144}] \cdot 3FL \cdot 13H_2O$ were built by adding 13 water molecules in the simulation cell. Nevertheless, ZL/1.5FL models containing 12 and 14 water molecules were also considered. The stabilization energies of the hydrated ZL/1.5FL models with respect to the isolated components were calculated with eq 2:

$$\begin{aligned}\Delta E(ZL \cdot 3FL \cdot xH_2O) \\ = E(ZL \cdot 3FL \cdot xH_2O) - E(ZL) - 3E(FL) - xE(H_2O)\end{aligned}\quad (2)$$

where $E(ZL \cdot 3FL \cdot xH_2O)$ is the energy of the optimized hydrated ZL/1.5FL model ($x = 12, 13, 14$) and $E(ZL)$ is the energy of the empty ZL, while $E(FL)$ and $E(H_2O)$ are respectively the energies of an isolated FL molecule and of an isolated water molecule calculated with the same simulation cell parameters. The relative stabilities of the systems with 12 and 14 water molecules with respect to that containing 13 H_2O 's, were calculated with eqs 3 and 4, respectively:

$$\begin{aligned}\Delta E(12/13) = E(ZL \cdot 3FL \cdot 12H_2O) - [E(ZL \cdot 3FL \cdot 13H_2O) \\ - E(H_2O)]\end{aligned}\quad (3)$$

$$\begin{aligned}\Delta E(14/13) = E(ZL \cdot 3FL \cdot 14H_2O) - [E(ZL \cdot 3FL \cdot 13H_2O) \\ + E(H_2O)]\end{aligned}\quad (4)$$

Stabilization energies and relative stabilities reported in the following are given in kJ per mol of simulation cell.

3. RESULTS AND DISCUSSION

3.1. TGA-MSEGA. Water and fluorenone contents in the ZL/FL composites were determined by TGA-MSEGA. Figure 3 shows the TG (a) and DTG curves (b) as a function of temperature for the as-synthesized ZL, for pure crystalline FL, and for the ZL/FL composites.

The as-synthesized ZL loses most of its water content (11.9%) in the 30–120 °C temperature range, with a maximum in the DTG curve at 110 °C. However, the weight loss keeps on up to 250 °C, as shown by the slight slope of the TGA curve. A water loss at such a low temperature is consistent with the ZL structure; in fact, among the 18 extraframework water molecules localized in the 12MR channel, only 5 are coordinated to K cations, while the remaining are weakly bonded to each other.^{26,39}

The thermal analysis of crystalline fluorenone (gray solid line in Figure 3) exhibits only one fast weight loss at 220 °C, and the mass spectrometry reveals that FL does not decompose in submoieties but is released in its molecular form.

As shown in Figure 3 and Table 2, in the four composites the water release occurs at about 100 °C and the weight losses are 8.7%, 7.3%, 5.5%, and 5.4% (corresponding to 13.6, 11.5, 8.8, and 8.8H₂O molecules per u.c.) in ZL/0.5FL, ZL/1.0FL, ZL/

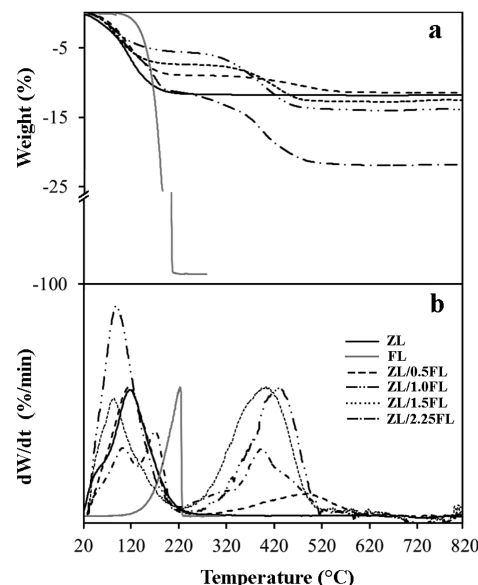


Figure 3. TG (a) and DTG curves (b) vs temperature for ZL (black solid curve), for pure FL (gray solid curve), and for the ZL/0.5FL (dashed black line), ZL/1.0FL (dashed-double dot black line), ZL/1.5FL (dotted black line), and ZL/2.25FL (dashed-dot black line) composites.

1.5FL, and ZL/2.25FL, respectively. The water loss temperature slightly decreases when the water amount in the composite decreases, as a consequence of the FL penetration. The fluorenone release in the composites occurs again in one step, but at higher temperature with respect to pure FL (in the range 300–500 °C). This indicates that FL is not simply physisorbed on the zeolite surface but is encapsulated inside the zeolite channels. It is worth noting that the release temperature decreases with increasing the FL loading, indicating an influence of loading on the host–guest FL–ZL interactions. The sample ZL/2.25FL shows a further weight loss at 170 °C, absent in the TG curve of all the other composites. This can be interpreted as the result of the removal of a portion of FL present as crystalline phase, not confined in zeolite porosities. This fact is confirmed by the XRPD pattern collected on that sample, showing reflections pertaining to the crystalline fluorenone phase (Figure 4).

On the basis of the mass spectrometry results, we observed that, when confined in the zeolite L, FL is released as CO₂ and C₆H₆ as a consequence of the higher release temperature. The weight losses corresponding to the encapsulated FL are 2.8%, 5.6%, 8.7%, and 9.5% (corresponding to 0.43, 0.88, 1.43, and 1.50 FL molecules) in the ZL/0.5FL, ZL/1.0FL, ZL/1.5FL, and ZL/2.25FL composites, respectively (Table 2). These results, and in particular the presence of only 1.5 molecules in the sample ZL/2.25FL, indicate that the maximum possible loading of the dye in zeolite L is 1.5 molecules per unit cell. The crystalline fluorenone detected in the case of the ZL/2.25FL composite corresponds to the exceeding dye on the zeolite surface. Consequently, this sample was not further investigated. In all of the investigated composites, the amounts of water and FL are, as expected, inversely correlated, indicating that the fluorenone molecules entering the channels replace the water molecules.

3.2. ATR-IR Spectroscopy. Figure 5 shows the IR spectra of FL in the solid state and in solution in cyclohexane (upper section “FL”) compared with the spectra of bare ZL (dotted

Table 2. Water Release Temperature, Water Weight Loss, and Number of Water Molecules per Unit Cell Determined by TGA-MSEGA (TGA) and by the Rietveld Refinement (R) for the ZL/FL Composites; and FL Release Temperature, FL Weight Loss, and Number of FL Molecules per Unit Cell Determined by TGA-MSEGA (TGA) and by the Rietveld Refinement (R) for the ZL/FL Composites

| sample | water loss T (°C) | water wt % | water (TGA) | water (R) | FL loss T (°C) | FL wt % | FL (TGA) | FL (R) |
|-----------|-------------------|------------|-------------|-----------|----------------|---------|----------|--------|
| ZL | 110 | 11.9 | 18 | 18 | | | | |
| ZL/0.5FL | 106 | 8.7 | 13.6 | 14.7 | 500 | 2.8 | 0.43 | 0.49 |
| ZL/1.0FL | 104 | 7.3 | 11.5 | 9.7 | 440 | 5.6 | 0.88 | 0.98 |
| ZL/1.5FL | 101 | 5.5 | 8.8 | 7.0 | 403 | 8.7 | 1.43 | 1.48 |
| ZL/2.25FL | 102 | 5.4 | 8.8 | | 400 | 9.5 | 1.50 | |

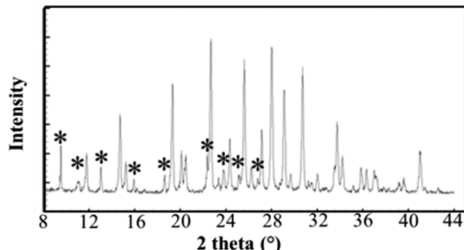


Figure 4. XRPD pattern of the ZL/2.25FL composite. The asterisks indicate the peaks of crystalline FL not adsorbed in ZL channels.

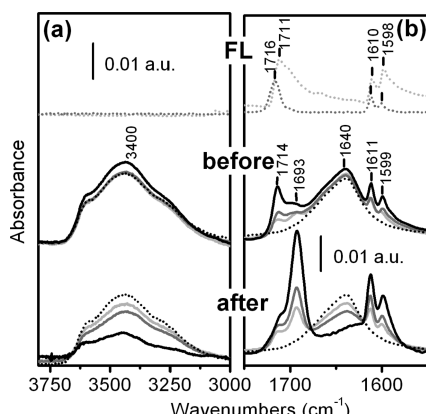


Figure 5. ATR-IR spectra, in the 3800–3000 and 1750–1500 cm^{-1} ranges of FL, ZL, and ZL/FL mixtures and composites. “FL” upper section: fluorenone in solid state (dotted light gray line) and in cyclohexane solution (dotted gray line). “Before” middle section: bare ZL (dotted black line) and ZL/FL mixtures before the thermal treatment, namely ZL/0.5FL (solid light gray), ZL/1.0FL (solid gray), and ZL/1.5FL (solid black line). “After” lower section: bare ZL (dotted black line, the same as above) and ZL/FL composites after thermal treatment, namely ZL/0.5FL (solid light gray), ZL/1.0FL (solid gray), and ZL/1.5FL (solid black line). Within the middle and lower sections, spectra have been normalized to the intensity of the ZL framework band centered at ca. 1005 cm^{-1} (see Figure S2 in the SI).

black line) and ZL mixed with FL before (middle section) and after (lower section) thermal treatment.

Among the IR signals, the stretching vibration of the carbonyl group of FL (at 1711 cm^{-1} in solid and 1716 cm^{-1} in cyclohexane solution) is expected to be particularly informative on the nature of the chemical environment around the FL molecule, being easily red-shifted if directly involved in interactions with positive charges (as in the case of FL grafting on K^+ ions). Conversely, the $\text{C}=\text{C}$ ring in plane stretching modes vibrating at 1610 and 1598 cm^{-1} are expected to be insensitive to the interaction of FL with the environment. The exposure of bare ZL to air for recording the IR spectrum

resulted in the adsorption of water molecules within the zeolite channels, as witnessed by the presence of the broad bands at 3400 and 1640 cm^{-1} , due to H_2O stretching and bending modes, respectively.⁶⁰ These spectral features remain essentially unchanged in the spectra of ZL simply mixed with FL (middle section), with this latter producing bands almost coincident with those of FL in the solid state. It is worthy of note that an additional weak component can be observed at 1693 cm^{-1} , which can be attributed to the $\text{C}=\text{O}$ group of FL interacting with positive charges,⁶¹ likely K^+ ions present on the external surface of zeolite crystals. Conversely, the band at 1693 cm^{-1} becomes the dominant $\nu\text{C}=\text{O}$ signal after thermal treatment of ZL/FL mixtures (lower section), while the H_2O band decreases in intensity. In particular, the presence of an isosbestic point between the 1640 and the 1693 cm^{-1} peaks is a clear indication that a diffusion of FL in the pores occurred, with dye molecules occupying positions no longer available for the adsorption of water molecules when the composites were exposed to air.

All the IR features of FL result to be strongly increased in intensity after the grafting, as expected for the introduction of the molecule in a strongly polarizing environment as the ZL pores. From these findings, it is evident that most of the FL molecules enter into the zeolite channels during the 120°C thermal treatment forming the ZL/FL composites. It is important to stress how the ATR-IR technique reveals its suitability to quickly and easily verify the grafting of dye molecules, bearing a functional group, as $\text{C}=\text{O}$, spectroscopically highly sensitive to the chemical environment.

3.3. Structure Refinement. As-Synthesized ZL Sample. The structure refinement of the as-synthesized ZL indicated the following extraframework species distribution (see Tables S1 and S3):

- (i) site KB—in the center of the cancrinite cage—is fully occupied and coordinated to six framework oxygen atoms;
- (ii) site KC—in the center of the 8MR channel parallel to the c axis, midway between the centers of two adjacent cancrinite cages—is fully occupied and coordinated by four oxygen atoms;
- (iii) site KD—in the main 12MR channel—is partially occupied and coordinated to six oxygen atoms and two water molecules.

The water content, corresponding to 18 molecules, is distributed over five extraframework sites located in the main channel, labeled WF, WH, WI, WJ, and WK. They are partially occupied and weakly bonded to the framework.

The XRPD patterns collected on ZL and on the ZL/FL composites show differences in the intensity of some diffraction peaks, with the most significant being related to the low 2θ angle region (Figure S1). It is well-known that, in zeolites, the

intensities of the low-angle peaks of the diffraction pattern are related to the extraframework species distribution. Thus, these changes are consistent with the FL penetration and in agreement with the TGA and ATR-IR results. Only small changes in the cell parameters occur; in particular, a slight increase of a and a decrease of c parameters are observed in the composites with respect to the original material (Table 1).

By comparing the results of the structural refinements of ZL with those of the three composites, slight deformations of both the channels running along the c axis can be observed by increasing the FL loading. In particular, the 12MR channel becomes more circular, while the 8MR one assumes a more elliptical shape (Figure 6). The combined effect of widening/contraction of the two channels justifies the minor variations in the unit cell parameters reported in Table 1.

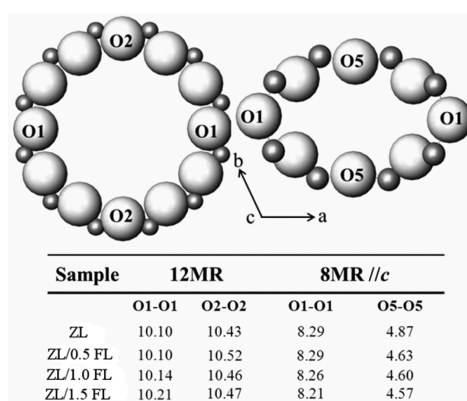


Figure 6. Dimensions of the 12MR and 8MR channels parallel to [001] before (ZL) and after the adsorption of fluorenone.

As regards the extraframework species, in all the studied samples, we observe a general disordered distribution of water and FL molecules on partially occupied positions. Only the extraframework sites KD, WI, and WJ undergo small coordinate changes, as a consequence of the dye penetration, as discussed in the following sections.

The structural refinements of the ZL/0.5FL and ZL/1.0FL composites gave similar results and are hence described together in the following section.

ZL/0.5FL and ZL/1.0FL Composites. The refinements revealed the presence of 0.49 and 0.98 FL molecules per unit cell in both ZL/0.5FL and ZL/1.0FL composites, respectively, in good agreement with the indications of the TGA analysis (Table 2). These molecules are sited on the mirror planes parallel to the c axis, statistically occupying one of the six equivalent positions—generated by the presence of the 6-fold axis parallel to [001] (Table S1, Figure 7a,b). In both composites, the oxygen of the carbonyl group (OFL) is oriented toward the two equivalent potassium sites (KD), located along the walls of the 12MR channel. The distances between OFL and KD (2.81(6) and 2.86(7) Å for the ZL/0.5 FL and ZL/1.0 FL composites, respectively) confirm that in both samples there is a strong interaction between these two atomic species, in keeping with the data of ATR-IR analysis (Figure 5).

Along with the dye, water molecules were also located in the 12MR channel: specifically, 14.7 molecules/u.c. in the ZL/0.5FL composite (distributed over the three independent partially occupied sites WH, WJ, and WI) and 9.7 molecules/u.c. in the ZL/1.0FL one (distributed over the two independent partially occupied sites WJ and WI) (Table S1). The OFL oxygen atom and C3 carbon occupy the same positions occupied by water molecules WI and WJ in ZL. These sites, hereafter labeled OFL/WI and C3/WJ (Tables S1 and S3), showed occupancy factors higher than those of the other carbon sites, hence suggesting a possible sharing of these positions by water molecules and FL atoms (Figure 7a,b). These results, in particular the higher amount of water in the less loaded sample, are in good agreement with what was found by TGA and IR analysis.

ZL/1.5FL Composite. From the refinement of the ZL/1.5FL composite, 1.48 FL molecules per unit cell were located, distributed over partially occupied sites, in line with the TGA analysis (Table 2). However, the disordered distribution of water and FL molecules greatly contributes to make the determination of the FL positioning/orientation from electronic density maps a very challenging task. Nevertheless, exploratory structure refinement attempts were performed by forcing the ZL framework 6-fold symmetry, and two FL orientations were found. The first (FL in Table S1, accounting for 0.5 molecules per unit cell) corresponds to the orientation found in the ZL/0.5FL and ZL/1.0FL composites. The second

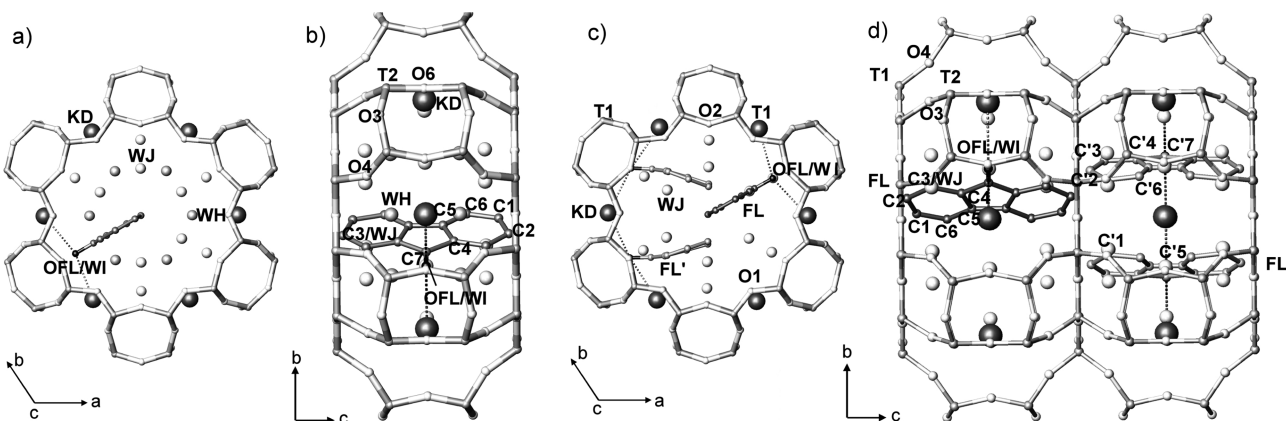


Figure 7. View along [001] and along [100] of the arrangement of the FL and water molecules in the ZL/0.5FL and ZL/1.0FL composites (a, b) and in the ZL/1.5FL composite (c, d), as obtained by Rietveld refinements. The positions of only one FL molecule in the ZL/0.5FL and ZL/1.0FL composites and of three (one FL and two FL') FL molecules in the ZL/1.5FL composite are represented for the sake of clarity.

(FL' in Table S1, accounting for 1.0 molecule per unit cell) features the FL molecular long axis parallel to the *c* axis, but with some atoms outside the mirror plane parallel to [001]. On the basis of the size and geometry of FL molecules, and considering the bond distances among the dye molecules obtained by the refinement, the only possible FL distribution is that reported in Figure 7c,d. In particular, if we consider two adjacent unit cells, one should be occupied by two equivalent nearly parallel FL' molecules (among the 12 symmetrically equivalent ones) while the other should contain one FL molecule. Also in this model every oxygen atom of the guest molecules is coordinated to two KD sites (Table S3).

As already observed in the ZL/0.5FL and ZL/1.0FL composites, the refinement located the water molecules in the OFL/WI and C3/WJ sites (Tables S1 and S3). The FL–water distances however showed values well below those expected from the corresponding van der Waals radii; e.g., the OFL' atom is at distances of 1.07 and 2.89 Å from WI and WJ, while C3' is at distances of 2.87 and 1.31 Å from WI and WJ. These short distances are due to the partial occupancy of the sites and to the great variability of the positions of the water molecules from unit cell to unit cell because of their dependence on the location of FL. Therefore, even though the *R/F²* value for this refinement may be considered rather good (8.7%) in view of the high number of variables, the 6-fold symmetry constraint imposed in the refinement resulted in a too short C–C distance (2.56 Å) between FL and FL' molecules present in two adjacent cells. To solve this structural inconsistency and provide a realistic structural model of the FL packing inside the composite, density functional calculations were performed.

3.4. Simulation Results. Modeling of Dry ZL/FL Adducts.

In order to try unraveling the structure of the FL organization in ZL nanochannels, let us first recall that the fluorenone molecular length, 8.9 Å along its longest axis, is greater than the ZL cell dimension along the channel (7.52 Å). FL is, however, noticeably shorter than the maximum channel opening (~12 Å), indicating that this dye could have orientation freedom inside the zeolite and should not necessarily align with the ZL channel axis. Actually, by increasing the FL content, a modest shortening of the cell along the *c* axis is detected, suggesting that, at high FL loading, an organization of the FL molecules in single file should be rather improbable. As reported in refs 36 and 37, at low loading (i.e., 0.5 FL per u.c.) the calculated minimum energy structure for a dry ZL/0.5FL system is characterized by a FL molecule coordinated, via the carbonyl oxygen, to a K⁺ cation and oriented with its long molecular axis forming an angle of about 30° with the *c* axis. The stabilization energy of this structure with respect to the isolated ZL and FL components amounts to -80.8 kJ mol⁻¹. Even though a geometry with the FL long axis aligned with the channel direction is only 12.1 kJ mol⁻¹ less stable than the minimum energy structure, at room temperature the FL most probable orientation is that with the molecular long axis at 30° with respect to the channel axis. Such an angle decreases to 20° upon hydration, indicating that in humid conditions not only FL keeps contact with K⁺ but also its average position and orientation inside the channel are not substantially influenced.^{36,37} Also, configurations with the FL long axis perpendicular to the channel axis, where the FL carbonyl oxygen is far from the extraframework potassium cations, are much higher in energy than those aligned with the channel axis

and become unstable at room temperature conditions, as evidenced by first-principles molecular dynamics.³⁷

Based on the above results and on host–guest structural properties, in the case of the ZL/1.0FL composite, the most probable supramolecular organization should feature the FL molecules approximately aligned with the channel axis and with their carbonyl oxygen directed toward the channel walls, where accessible K⁺ ions are located. With this in mind, two kinds of arrangements, described as (2,0) or (1,1), could be devised, corresponding to (i) two adjacent ZL unit cells approximately occupied by two and 0 FL molecules (2,0); (ii) each ZL unit cell containing 1 FL molecule (1,1). Two different orientations of the C=O group of the two FL molecules were considered: (i) anti, characterized by an antiparallel arrangement of the C=O groups; (ii) sin, where the C=O groups are parallel. Geometry optimization of several ZL/1.0FL models exhibiting these arrangements indicates that different optimized structures have comparable energies, separated by less than 4 kJ mol⁻¹ (see Figure 8). The most stable structure is an anti-(2,0)

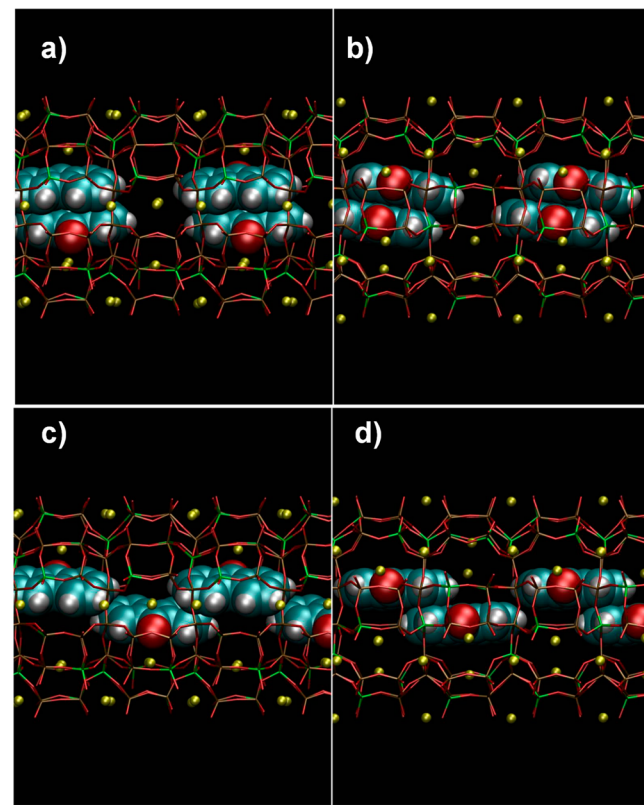


Figure 8. Graphical representation of minimum energy structures calculated for the ZL/1.0FL models: (a) anti-(2,0) arrangement of the FL molecules; (b) sin-(2,0) arrangement; (c) anti-(1,1) arrangement; (d) sin-(1,1) arrangement. ZL framework atoms are represented as sticks (brown: Si, green: Al, red: O), K⁺ as yellow spheres. FL atoms are in the van der Waals representation (cyan: C, red: O, white: H).

configuration (Figure 8a) and has a stabilization energy of -141.4 kJ mol⁻¹ with respect to the isolated components (see eq 1). A sin-(2,0) arrangement (Figure 8b) is, however, nearly isoenergetic, being less stable than the minimum energy structure by only 5.0 kJ mol⁻¹. Also, an anti-(1,1) structure (Figure 8c) is of comparable energy, being only 3.8 kJ mol⁻¹ less stable than the anti-(2,0) one. On the other hand, the most stable among the sin-(1,1) arrangements (Figure 8d) is 33.5 kJ

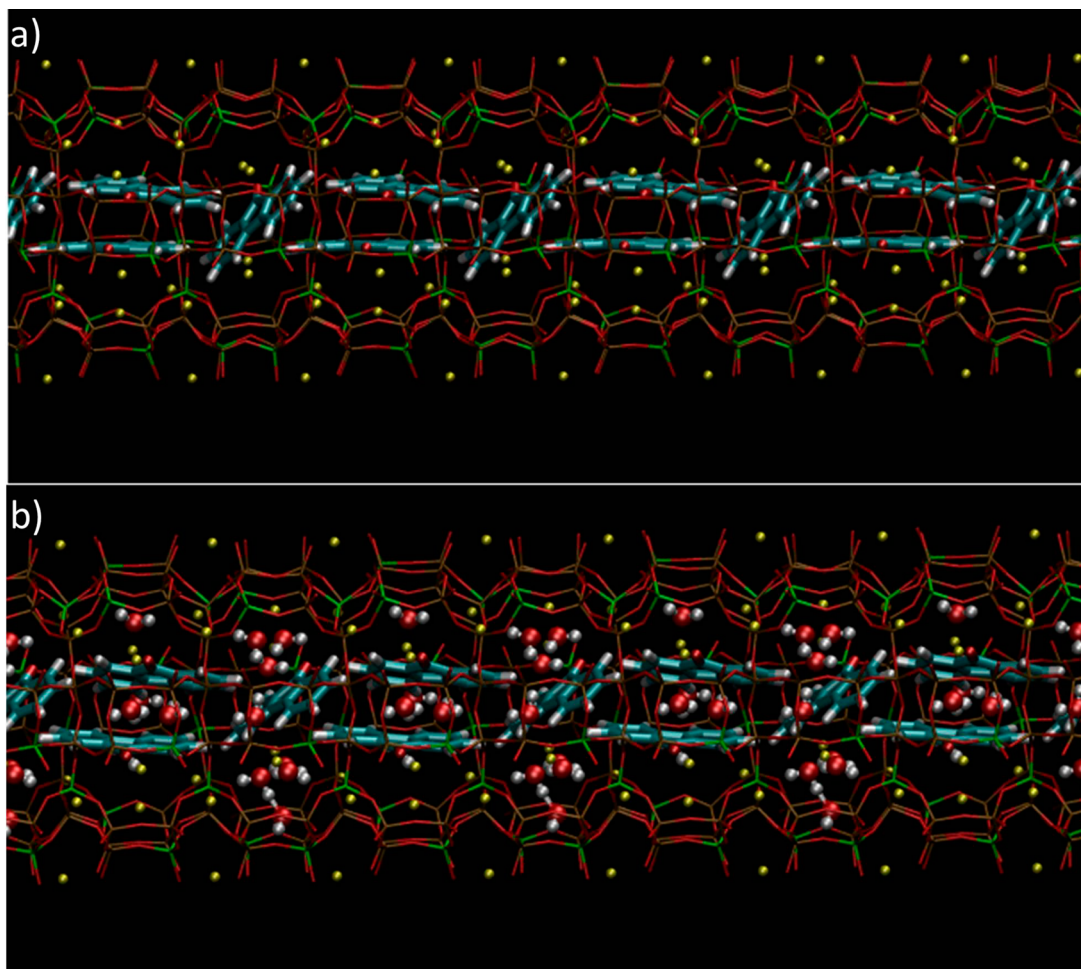


Figure 9. Graphical representation of the minimum energy structure calculated for the (a) dry ZL/1.5FL model; (b) hydrated ZL/1.5FL model (with 13H₂O in the simulation cell). Atom color codes as in Figure 8.

mol⁻¹ higher in energy than the anti-(2,0). Since all of these structures are characterized by distances between the FL carbonyl oxygen and K⁺ in line with the corresponding experimental values and compatible with a strong potassium–FL interaction, their different relative stabilities mainly derive from FL–FL interactions. Actually, the minimum energy structure for the ZL/1.0 FL system is just the one characterized by the highest degree of FL close-packing, which maximizes the favorable van der Waals interactions between the dye molecules.

Also, for the maximum loading of 1.5 FL per u.c., we performed geometry optimization on different guess structures, all characterized by a (2,1) FL arrangement (see Figure 9a). The stabilization energy of the resulting minimum energy structure with respect to the isolated components (eq 1) amounts to $-266.5 \text{ kJ mol}^{-1}$. Here the supramolecular organization consists of two FL molecules, FL1 and FL2 (in a sin configuration), located approximately inside one of the ZL unit cells with their long axes nearly parallel to each other and to the channel direction, while the third one, FL3, is positioned in the adjacent unit cell and oriented at about 45° with respect to the ZL channel axis. Indeed, the stronger intermolecular interactions and the severe structural constraints implied by confinement in nanochannels at high packing conditions force the FL molecules to organize just like a ladder with inclined rungs running along the ZL channel, as clearly evidenced in

Figure 9. Indeed, the molecules are essentially planar and show only slight distortions from the ideal gas-phase FL structure, indicating that this ladderlike supramolecular architecture is achieved without any significant perturbation of the FL molecular geometry. Moreover, the FL nanoladder still maintains some resemblance to the structure of the FL crystal,³⁸ suggesting that, at high loading regimes, also guest–guest van der Waals interactions, and specifically π–π stacking, are pivotal in governing supramolecular organization. The confining environment provided by the ZL nanochannels prevents the formation of the thermodynamically stable bulk solid FL and constrains the dye molecules to self-assemble into a new, low-dimensionality solid phase: the FL nanoladder. Nevertheless, such a stunning example of spatio-morphologically controlled crystallization owes its existence also to noncovalent though directional host–guest interactions, which drive the positioning and orientation of each individual dye molecule forming the nanoladder. In this respect, we notice that each FL is in close contact with the ZL K⁺ cations via its carbonyl oxygen, in line with the previously discussed experimental evidence. More specifically, the distances of the three carbonyl oxygens from the zeolite K⁺ cations amount to 2.539, 2.570, and 2.676 Å, respectively, indicating that, like in the case of lower FL-loading ZL/FL systems,^{36,37} also strong C=O/K⁺ interactions play a key role in supramolecular organization.

Hydrated System with 1.5 FL per u.c. Several hydrated models of the ZL/1.5FL system were considered, characterized either by a different number of water molecules in the simulation cell (in the 12–14 range) or by a different starting arrangement of the FL and H₂O molecules. The minimum energy structure obtained by placing 13 water molecules in the simulation cell is shown in Figure 9b. In this structure, 8 water molecules are located in the unit cell containing FL3 and the remaining 5 in that occupied by the FL1 and FL2 molecules. In line with results obtained on other dye–ZL composites,^{35,54} the water molecules are mainly clustered in the ZL channel region characterized by a lower local concentration of the dye and try to adopt a quasi-tetrahedral organization mimicking that of water in the condensed phases, in order to maximize the number and strength of hydrogen bonds. Indeed, the high value of the stabilization energy calculated for this structure, 752.7 kJ mol⁻¹ (eq 2), indicates that water actively contributes to stabilize close-packing of dye molecules inside zeolite nanochannels. As clearly evidenced in Figure 9, besides slight deformations related to the water copresence, the arrangement of the FL molecules resembles quite closely the FL nanoladder found in the dry ZL/1.5FL composite. It can therefore be concluded that, at ambient temperature and pressure conditions, water molecules do not significantly perturbate the FL supramolecular organization. This finding is nicely in line with the fact that FL molecules interact more strongly with the zeolite than water does, as demonstrated in ref 36. Due to the dominant FL–K⁺ interaction, water molecules cannot displace the dye from the zeolite, but they seamlessly incorporate FL molecules into the hydrogen bond network and finely tune FL positioning and orientation inside the ZL channel through hydrogen bond interactions. Actually, the distances of the three carbonyl oxygens from the zeolite K⁺ cations, amounting to 2.524, 2.590, and 2.848 Å respectively, are very close to those of the dry ZL/1.5FL system, confirming that the presence of water has only minor structural effects on the FL arrangement. As far as the water content is concerned, by applying eqs 3 and 4, we calculated that the system containing 13 H₂O (namely, 6.5 H₂O per crystallographic cell) is more stable than both the systems containing 12 or 14 water molecules, by 149.4 and 38.5 kJ mol⁻¹, respectively. The greater energy stability of the 13 H₂O composite, with respect to the 12 H₂O one, can be easily rationalized on the basis of the higher number of hydrogen bond interactions. Nevertheless, the minimum energy structure obtained at higher water content (14 H₂O) is less stable than the 13 H₂O one because, as a result of the reduced available space inside the ZL channel, the geometry of the FL molecules exhibits larger distortions from the ideal planar FL structure. Therefore, computational results, besides integrating experimental data on the high-FL-content composite, shed light and rationalize several aspects of supramolecular organization inside ZL channels, thus enabling us, for the first time, to catch a fleeting glimpse of how promisingly appealing it could be to explore close-packed dye molecules self-assembled in 1-D confining environments.

4. CONCLUSIONS

To unravel the supramolecular organization of close-packed photoactive molecules confined in one-dimensional nanochannels, zeolite L/fluorenone (ZL–FL) composites characterized by different dye loading have been synthesized. Results of thermogravimetric, IR, and X-ray structural refinements established that the maximum degree of FL loading

corresponds to 1.5 FL molecules per ZL unit cell. A thorough characterization of the structural properties and energetics of this dye–zeolite system has been accomplished by DFT-based modeling, which revealed the template-directed self-assembly of planar dye molecules into a noncovalent nanoladder.

By increasing loading from 0 to 1.5 molecules per cell, fluorenone gradually replaces water molecules in ZL in view of its stronger interaction with the zeolite and fills the nanochannel by organizing into arrangements that concomitantly maximize the π-stacking (intermolecular guest–guest interactions) and allow each FL carbonyl group to interact with a K⁺ (host–guest interactions). Such organized FL distributions only at maximum loading can be considered as a single, continuous nanostructure of dye molecules. This arrangement, formed by pairs of π-stacked molecules connected by a single FL, holds some resemblance with the structure of solid fluorenone (the FL pairs); however, the confinement inside ZL channels and the different dimensions of the FL molecule and ZL unit cell prevent the connectivity of consecutive pairs of molecules like in crystalline fluorenone, thus resulting in the formation of a unique architecture. Interestingly, the progressive filling of FL is accompanied by slight though appreciable deformations of the channel apertures, indicating that also zeolite framework flexibility contributes to achieve the optimal FL organization (i.e., that characterized by the highest stability) at the maximum loading. Moreover, the water molecules inside the channel after FL intrusion are arranged in such a way to maximize hydrogen bond interaction, thus providing further stabilization to the system without altering the FL distribution, which is governed by the stronger FL–FL and FL–ZL interactions.

On the whole, all of the results presented in this study highlight the key role of the ZL channels in providing spatial, directional, and morphological control over the realization of supramolecular nanoarchitectures of photoactive species and stress the relevance of extraframework K⁺ cations in stabilizing carbonyl-functionalized species inside ZL and in fine-tuning their organization.

Among the ZL/FL composites investigated in this study, only the maximally loaded system features a continuous and organized distribution of dye molecules inside ZL nanochannels. By virtue of this architecture, the ZL/1.5FL composite should be the most promising candidate for technological applications. Following this hypothesis, future work specifically aimed at electronic and optical properties of close-packed ZL/FL composites will essentially focus on the maximally loaded system. Nevertheless, the identification of the first continuous and *quasi* 1-D dye nanostructure self-assembled into a zeolite, accompanied by the understanding of the interplay of host–guest/guest–guest interactions governing supramolecular organization at the high packing conditions gathered in this study, strongly suggests that high-loading regimes are promising and deserve to be deeply investigated, giving thus further momentum to the design of dye–ZL composites for innovative optical devices.

■ ASSOCIATED CONTENT

Supporting Information

Observed and calculated diffraction patterns and final difference curve from Rietveld refinements of the pure ZL and of the ZL/0.5FL, ZL/1.0FL, ZL/1.5FL composites. ATR-IR spectra of bare ZL and ZL/FL materials before and after the thermal treatment. Atomic coordinates, occupancy factors, and thermal

displacement parameters for the bare ZL, ZL/0.5FL, ZL/1.0FL, and ZL/1.5FL composites. Framework bond distances for the ZL and ZL/0.5FL, ZL/1.0FL, and ZL/1.5FL composites. Extraframework bond distances for ZL, ZL/0.5FL, ZL/1.0FL, and ZL/1.5FL composites. This material is available free of charge via the Internet at <http://pubs.acs.org>.

AUTHOR INFORMATION

Corresponding Author

*E-mail: gloria.tabacchi@uninsubria.it.

Present Address

○(G.A.) European Synchrotron Radiation Facility (ESRF), B.P. 220, 38043 Grenoble, France.

Notes

The authors declare no competing financial interest.

ACKNOWLEDGMENTS

The BM01 beamline at the European Synchrotron Radiation Facility and Dr. Vladimir Dmitriev are acknowledged for allocation of experimental beamtime. Dr. Simona Bigi and Dr. Daniele Malferrari are acknowledged for the help in TGA-MSEGA analyses. Professor Gion Calzaferri is acknowledged for useful discussions. Prof. Carlo Lamberti is acknowledged for the hospitality at NIS laboratories. This work was supported by the Italian MIUR, within the framework of the following projects: PRIN2009 “Struttura, microstruttura e proprietà dei minerali”; PRIN2010-11 “Dalle materie prime del sistema Terra alle applicazioni tecnologiche: studi cristallochimici e strutturali”; FIRB, Futuro in Ricerca “ImPACT” (RBFR12CLQD); INFOCHEM project PRIN 2010CX2TLM_006.

REFERENCES

- (1) Calzaferri, G. Nanochannels: Hosts for the Supramolecular Organization of Molecules and Complexes. *Langmuir* **2012**, *28*, 6216–6231.
- (2) Calzaferri, G.; Lutkouskaya, K. Mimicking the Antenna System of Green Plants. *Photochem. Photobiol. Sci.* **2008**, *7*, 879–910.
- (3) Calzaferri, G.; Méallet-Renault, R.; Brühwiler, D.; Pansu, R.; Dolamic, I.; Dienel, T.; Adler, P.; Li, H.; Kunzmann, A. Designing Dye-Nanochannel Antenna Hybrid Materials for Light Harvesting, Transport and Trapping. *ChemPhysChem* **2011**, *12*, 580–594.
- (4) Grüner, M.; Siozios, V.; Hagenhoff, B.; Breitenstein, D.; Strassert, C. A. Structural and Photosensitizing Features of Phthalocyanine—Zeolite Hybrid Nanomaterials. *Photochem. Photobiol.* **2013**, *89*, 1406–1412.
- (5) Tsotsalas, M. M.; Kopka, K.; Luppi, G.; Wagner, S.; Law, M. P.; Schafers, M.; De Cola, L. Encapsulating (111)In in Nanocontainers for Scintigraphic Imaging: Synthesis, Characterization, and in Vivo Biodistribution. *ACS Nano* **2010**, *4*, 342–348.
- (6) Li, Z.; Luppi, G.; Geiger, A.; Josel, H.-P.; De Cola, L. Bioconjugated Fluorescent Zeolite L Nanocrystals as Labels in Protein Microarrays. *Small* **2011**, *7*, 3193–3201.
- (7) El-Gindi, J.; Benson, K.; De Cola, L.; Galla, H.-J.; Kehr, N. S. Cell Adhesion Behaviour on Enantiomerically Functionalized Zeolite L Monolayers. *Angew. Chem., Int. Ed.* **2012**, *51*, 3716–3720.
- (8) Wen, T.; Zhang, W.; Hu, X.; He, L.; Li, H. Insight into the Luminescence Behavior of Europium(III) β -Diketonate Complexes Encapsulated in Zeolite L Crystals. *ChemPlusChem* **2013**, *78*, 438–442.
- (9) Szarpak-Jankowska, A.; Burgess, C.; De Cola, L.; Huskens, J. Cyclodextrin-Modified Zeolites: Host–Guest Surface Chemistry for the Construction of Multifunctional Nanocontainers. *Chem.—Eur. J.* **2013**, *44*, 14925–14930.
- (10) Manzano, H.; Gartzia-Rivero, L.; Bañuelos, J.; López-Arbeloa, I. Ultraviolet-Visible Dual Absorption by a Single BODIPY Dye Confined in LTL Zeolite Nanochannels. *J. Phys. Chem. C* **2013**, *117*, 13331–13336.
- (11) Caro, J.; Marlow, F.; Wüst, M. Chromophore–Zeolite Composites—The Organizing Role of Molecular-Sieves. *Adv. Mater.* **1994**, *6*, 413–416.
- (12) Ihlein, G.; Schuth, F.; Kraus, O.; Vietze, U.; Laeri, F. Alignment of a Laser Dye in the Channels of the AlPO₄-5 Molecular Sieve. *Adv. Mater.* **1998**, *10*, 1117–1119.
- (13) Hoppe, R.; Schulz-Ekloff, G.; Wöhrle, D.; Kirschhock, C.; Fuess, H.; Utterhoeven, L.; Schoonheydt, R. Incorporation of Methylene Blue in NaY Zeolite at Crystallographically Defined Positions. *Adv. Mater.* **1995**, *7*, 61–64.
- (14) Calzaferri, G.; Pauchard, M.; Maas, H.; Huber, S.; Khatyr, A.; Schaafsma, T. J. Photonic Antenna System for Light Harvesting, Transport and Trapping. *Mater. Chem.* **2002**, *12*, 1–13.
- (15) Mahato, R. N.; Lülf, H.; Siekman, M. H.; Kersten, S. P.; Bobbert, P. A.; de Jong, M. P.; De Cola, L.; van der Wiel, W. G. Ultrahigh Magnetoresistance at Room Temperature in Molecular Wires. *Science* **2013**, *341*, 257–260.
- (16) Onida, B.; Bonelli, B.; Lucco-Borlera, M.; Flora, L.; Otero Arean, C.; Garrone, E. Spectroscopic Properties of Dye-Loaded Mesoporous Silicas of the Structural Type MCM-41. *Stud. Surf. Sci. Catal.* **2001**, *135*, 364–364.
- (17) Busby, M.; Blum, C.; Tibben, M.; Fibikar, S.; Calzaferri, G.; Subramaniam, V.; De Cola, L. Time, Space, and Spectrally Resolved Studies on J-Aggregate Interactions in Zeolite L Nanochannels. *J. Am. Chem. Soc.* **2008**, *130*, 10970–10976.
- (18) Kim, H. S.; Pham, T. T.; Yoon, K. B. Aligned Inclusion of Dipolar Dyes into Zeolite Channels by Inclusion in the Excited State. *J. Am. Chem. Soc.* **2008**, *130*, 2134–2135.
- (19) Martínez-Martínez, V.; García, R.; Gómez-Hortigüela, L.; Sola Llano, R.; Pérez-Pariente, J.; López-Arbeloa, I. Highly Luminescent and Optically Switchable Hybrid Material by One Pot Encapsulation of Dyes into MgAPO-11 Unidirectional Nanopores. *ACS Photonics* **2014**, DOI: 10.1021/ph4000604.
- (20) Li, P.; Wang, Y.; Li, H.; Calzaferri, G. Luminescence Enhancement after Adding Stoppers to Europium(III) Nano zeolite L. *Angew. Chem., Int. Ed.* **2014**, *53*, 2904–2909.
- (21) Devaux, A.; Calzaferri, G.; Miletto, I.; Cao, P.; Belser, P.; Brühwiler, D.; Khorev, O.; Häner, R.; Kunzmann, A. Self-Absorption and Luminescence Quantum Yields of Dye–Zeolite L Composites. *J. Phys. Chem. C* **2013**, *117*, 23034–23047.
- (22) Calzaferri, G.; Huber, S.; Maas, H.; Minkowski, C. Host-Guest Antenna Materials. *Angew. Chem., Int. Ed.* **2003**, *42*, 3732–3758.
- (23) Devaux, A.; Minkowski, C.; Calzaferri, G. Electronic and Vibrational Properties of Fluorenone in the Channels of Zeolite L. *Chem.—Eur. J.* **2004**, *10*, 2391–2408.
- (24) Calzaferri, G.; Devaux, A. In *Supramolecular Photochemistry*; Ramamurthy, V., Inoue, Y., Eds.; Wiley&Sons: 2011.
- (25) Lupulescu, A. I.; Kumar, M.; Rimer, J. D. A Facile Strategy to Design Zeolite L Crystals with Tunable Morphology and Surface Architecture. *J. Am. Chem. Soc.* **2013**, *135*, 6608–6617.
- (26) Barrer, R. M.; Villiger, H. The Crystal Structure of the Synthetic Zeolite L. *Z. Kristallogr.* **1969**, *128*, 352–370.
- (27) Lee, Y. J.; Lee, J. S.; Yoon, K. B. Synthesis of Long Zeolite-L Crystals with Flat Facets Original Research Article. *Microporous Mesoporous Mater.* **2005**, *80*, 237–246.
- (28) Hennessy, B.; Megelski, S.; Marcolla, C.; Shklover, V.; Bärlocher, Ch.; Calzaferri, G. Characterization of Methyl Viologen in the Channels of Zeolite L. *J. Phys. Chem. B* **1999**, *103*, 3340–3351.
- (29) Simoncic, P.; Armbruster, T.; Pattison, P. Cationic Thionin Blue in the Channels of Zeolite Mordenite. *J. Phys. Chem. B* **2004**, *108*, 17352–17360.
- (30) Calzaferri, G. Energy Transfer Processes in Nanochannels. *Il Nuovo Cimento* **2008**, *123 B*, 1337–1367.
- (31) Huber, S.; Zabala Ruiz, A.; Li, H.; Patrinoiu, G.; Botta, C.; Calzaferri, G. Optical Spectroscopy of Inorganic-Organic Host-Guest Nanocrystals Organized as Oriented Monolayers. *Inorg. Chim. Acta* **2007**, *360*, 869–875.

- (32) Blum, C.; Cesa, Y.; Escalante, M.; Subramaniam, V. Multimode Microscopy: Spectral and Lifetime Imaging. *J. R. Soc. Interface* **2009**, *6*, S35–S43.
- (33) Megelski, S.; Lieb, A.; Pauchard, M.; Drechsler, A.; Glaus, S.; Debus, C.; Meixner, A. J.; Calzaferri, G. Orientation of Fluorescent Dyes in the Nano Channels of Zeolite L. *J. Phys. Chem. B* **2001**, *105*, 25–35.
- (34) Gasecka, A.; Dieu, L.-Q.; Brühwiler, D.; Brasselet, S. Probing Molecular Order in Zeolite L Inclusion Compounds Using Two-Photon Fluorescence Polarimetry. *J. Phys. Chem. B* **2010**, *114*, 4192–4198.
- (35) Fois, E.; Tabacchi, G.; Calzaferri, G. Orientation and Order of Xanthene Dyes in the One-Dimensional Channels of Zeolite L: Bridging the Gap between Experimental Data and Molecular Behavior. *J. Phys. Chem. C* **2012**, *116*, 16784–16799.
- (36) Fois, E.; Tabacchi, G.; Calzaferri, G. Interactions, Behavior and Stability of Fluorenone Inside Zeolite Nanochannels. *J. Phys. Chem. C* **2010**, *114*, 10572–10579.
- (37) Zhou, X.; Wesolowski, T. A.; Tabacchi, G.; Fois, E.; Calzaferri, G.; Devaux, A. First-Principles Simulations of Absorption Bands of Fluorenone in Zeolite L. *Phys. Chem. Chem. Phys.* **2013**, *15*, 159–167.
- (38) Luss, H. R.; Smith, D. L. The Crystal and Molecular Structure of 9-Fluorenone. *Acta Crystallogr., B* **1972**, *28*, 884–889.
- (39) Gigli, L.; Arletti, R.; Quartieri, S.; Di Renzo, F.; Vezzalini, G. The High Thermal Stability of the Synthetic Zeolite KL: Dehydration Mechanism by in Situ SR-XRPD Experiments. *Microporous Mesoporous Mater.* **2013**, *177*, 8–16.
- (40) Hammersley, A. P.; Svensson, S. O.; Hanfland, M.; Fitch, A. N.; Häusermann, D. Two Dimensional Detector Software: From Real Detector to Idealized Image or Two Theta Scan. *High Pressure Res.* **1996**, *14*, 235–248.
- (41) Larson, A. C.; Von Dreele, R. B. *General Structure Analysis System "GSAS"*; Los Alamos National Laboratory Report; Los Alamos, 1994; LAUR 86-748.
- (42) Toby, B.H. J. EXPGUI, a Graphical User Interface for GSAS. *Appl. Crystallogr.* **2001**, *34*, 210–213.
- (43) Perdew, J. P.; Burke, K.; Ernzerhof, M. Generalized Gradient Approximation Made Simple. *Phys. Rev. Lett.* **1996**, *77*, 3865–3868.
- (44) Grimme, S. Semiempirical GGA-Type density Functional Constructed with a Long-Range Dispersion Correction. *J. Comput. Chem.* **2006**, *27*, 1787–1799.
- (45) Vanderbilt, D. Soft self-Consistent Pseudopotentials in a Generalized Eigenvalue Formalism. *Phys. Rev. B* **1990**, *41*, 7892–7895.
- (46) Kleinman, L.; Bylander, D. M. Efficacious Form for Model Pseudopotentials. *Phys. Rev. Lett.* **1982**, *48*, 1425–1428.
- (47) Hamman, D. R.; Schlüter, M.; Chiang, C. Norm-Conserving Pseudopotentials. *Phys. Rev. Lett.* **1979**, *43*, 1494–1497.
- (48) Troullier, N.; Martins, J. L. Efficient pseudopotentials for Plane-Wave Calculations. *Phys. Rev. B* **1991**, *43*, 1993–2006.
- (49) Gamba, A.; Tabacchi, G.; Fois, E. TS-1 from First Principles. *J. Phys. Chem. A* **2009**, *113*, 15006–15015.
- (50) Ceriani, C.; Fois, E.; Gamba, A.; Tabacchi, G.; Ferro, O.; Quartieri, S.; Vezzalini, G. Dehydration Dynamics of Bikitaite: Part II. Ab Initio Molecular Dynamics Study. *Am. Mineral.* **2004**, *89*, 102–109.
- (51) Spanò, E.; Tabacchi, G.; Gamba, A.; Fois, E. On the Role of Ti(IV) as a Lewis Acid in the Chemistry of Titanium Zeolites: Formation, Structure, Reactivity, and Aging of Ti-Peroxo oxidizing Intermediates. A First Principles Study. *J. Phys. Chem. B* **2006**, *110*, 21651–21661.
- (52) Fois, E.; Gamba, A.; Tabacchi, G. Bathochromic Effects in Electronic Excitation Spectra of Hydrated Ti Zeolites: A Theoretical Characterization. *ChemPhysChem* **2008**, *9*, 538–543.
- (53) Fois, E.; Tabacchi, G.; Barreca, D.; Gasparotto, A.; Tondello, E. “Hot” Surface Activation of Molecular Complexes: Insight from Modeling Studies. *Angew. Chem., Int. Ed.* **2010**, *49*, 1944–1948.
- (54) Fois, E.; Tabacchi, G.; Devaux, A.; Belser, P.; Brühwiler, D.; Calzaferri, G. Host–Guest Interactions and Orientation of Dyes in the One-Dimensional Channels of Zeolite L. *Langmuir* **2013**, *29*, 9188–9198.
- (55) CPMD Code: MPI für Festkörperforschung: Stuttgart, Germany; IBM Zürich Research Laboratory: Zürich, Switzerland, 1990–2012.
- (56) Fois, E.; Tabacchi, G.; Quartieri, S.; Vezzalini, G. Dipolar Host/Guest Interactions and Geometrical Confinement at the Basis of the Stability of One-Dimensional Ice in Zeolite Bikitaite. *J. Chem. Phys.* **1999**, *111*, 355–359.
- (57) Fois, E.; Gamba, A.; Tabacchi, G.; Quartieri, S.; Vezzalini, G. Water Molecules in Single File: First-Principles Studies of One-Dimensional Water Chains in Zeolites. *J. Phys. Chem. B* **2001**, *105*, 3012–3016.
- (58) Fois, E.; Gamba, A.; Tabacchi, G.; Quartieri, S.; Vezzalini, G. On the Collective Properties of Water Molecules in One-Dimensional Zeolitic Channels. *Phys. Chem. Chem. Phys.* **2001**, *3*, 4158–4163.
- (59) Fois, E.; Gamba, A.; Medici, C.; Tabacchi, G. Intermolecular Electronic Excitation Transfer in a Confined Space: A First-Principles Study. *ChemPhysChem* **2005**, *6*, 1917–1922.
- (60) Pazé, C.; Bordiga, S.; Lamberti, C.; Salvalaggio, M.; Zecchina, A.; Bellussi, G. Acidic Properties of H- β Zeolite As Probed by Bases with Proton Affinity in the 118–204 kcal mol⁻¹ Range: A FTIR Investigation. *J. Phys. Chem. B* **1997**, *101*, 4740–4751.
- (61) Zecchina, A.; Scarano, D.; Bordiga, S.; Spoto, G.; Lamberti, C. Surface Structures of Oxides and Halides and Their Relationships to Catalytic Properties. *Adv. Catal.* **2002**, *46*, 265–397.